Impact of impurity radiation locations on the plasma performance at W7-X stellarator

D. Zhang[1], R. Burhenn[1], P. Hacker[1], F. Reimold[1], L. Giannone[2], S. Kwak[1], R. Laube[1], J. Svensson[1], F. Penzel[2], J. Baldzuhn[1], C.D. Beidler[1], M. Beurskens[1], S. Bozhenkov[1], S. Brezinsek[3], K.J. Brunner[1], R. Bussiahn[1], B. Buttenschön[1], Y. Feng[1], G. Fuchert[1], Y. Gao[3], O. Grulke[1], U. Höfel[1], M. Hirsch[1], Z. Huang[4], M. Jakubowski[1], J. Knauer[1], R. König[1], M. Krychowiak[1], H.P. Laqua[1], A. Langenberg[1], H. Niemann[1], N. Pablant[5], A. Pavone[1], E. Pasch[1], K. Rahbarnia[1] , A. Stechow[1], N. Tamura[6] , H. Thomsen[1] and the W7-X team*

[1]Max-Planck-Institut für Plasmaphysik, 17489 Greifswald Germany
[2]Max-Planck-Institut für Plasmaphysik, 85748 Garching, Germany
[3]Forschungszentrum Jülich GmbH, IEK-4 D-52425 Jülich, Germany
[4]Plasma Science and Fusion Center, MIT, Cambridge, MA 02139, USA
[5]Princeton Plasma Physics Laboratory, Princeton, NJ, US
[6]National Institute for Fusion Science, Gifu 509-5292, JAPAN
**T. Klinger et al., Nuclear Fusion 59 (2019) 112004 doi: 10.1088/1741-4326/ab03a7*

1. Introduction The optimized stellarator Wendelstein 7-X (W7-X) has recently conducted its first divertor operation. One of the main scientific objectives is to examine and optimize the island divertor as a potential concept for a future stellarator reactor. One promising approach is to keep the impurities released from the plasma-surface interaction region in the scrape-off layer (SOL) in order to prevent both impurity contamination and possible degradation of the core plasma and at the same time to reduce the heat load on the divertors by edge impurity radiation. The search for optimized operation conditions, allowing for both, high-radiation and high plasma performance, is therefore of great concern to us.

2. Experiment description W7-X is currently the largest advanced stellarator worldwide with major radius of 5.5 m, effective minor radius ~0.5 m and plasma volume ~30 m^3. The plasma facing components consist of the graphite-covered divertor modules and wall protections as well as stainless-steel wall. Turbomolecular pumps allow control of the machine vacuum. Glow- and ECR-heated He-discharges are used for machine conditioning. Boronisation has been performed for the first time during the operation phase OP1.2b in 2018 [1]. Intrinsic impurities are mainly low-Z elements, such as carbon and oxygen. The experiments described here were carried out in 'standard' magnetic configuration (B_0 = 2.5 T) with a 5/5 island chain at the edge. The island dimension is radially around 6.5 cm. The plasma considered here is generated using X2-mode electron cyclotron resonance heating (ECRH).

The experimental results are based on the following diagnostics: a two-camera bolometer system installed at a triangular cross-section (with a spatial resolution of 3-4 cm) for measuring the plasma radiation [2]. The total radiated power loss, P_{rad}, is a linear extrapolation of the radiation in the observation volume (calculated based on the line-integrated signals) to the whole plasma volume ignoring toroidal variations. Additional 10µm-Be-covered channels (called later SXR-bolometer) provide radiation loss in the soft-x-ray (> 1 keV) range. Other plasma diagnostics involved [3-7] are: an interferometer for measuring the line-averaged plasma density $<n_e>$, the magnetic diagnostic for the plasma stored energy W_p, ECE (electron cyclotron emission) radiometers or Thomson-scattering system for the electron temperature, target plate thermography for heat loads (P_{div}) measurements, and spectroscopic diagnostics for monitoring impurity ion radiations and bremsstrahlung radiation.

3. Experimental results In the pre-boronisation experiments, a quasi-stationary highly radiative divertor plasma regime has been observed in a hydrogen plasma in which the value of P_{rad} approaches the absorbed heating power P_{ECRH} (~3 MW) after pellet injections. Complete power detachment without significant confinement degradation has been achieved at a critical density of $<n_e> = 2.2\ 10^{19}\ m^{-3}$ [8]. Oxygen radiation, which is edge-localized, plays here a predominant role. After boronisation, impurity radiation (especially from oxygen) decreases noticeably [7]; P_{rad} is reduced by a factor of 6 under similar experimental conditions. Consequently, the high-radiation regime with plasma detachment could be achieved at higher density [9]. We examine the plasma performances for selected discharges in post-boronisation experiments paying attention to the radiation loss fraction inside the last closed flux surface (LCFS) $f_{rad,core}$, defined as $f_{rad,core}=1-P_{rad,SOL}/P_{rad}$, with $P_{rad,SOL}$ standing for the radiated power loss from the SOL measured by those bolometer channels purely monitoring the SOL-region.

3.1 Radially inward shift of radiation zone at detachment transition Plasma radiation features are recently analyzed for a 2 MW ECR-heated hydrogen discharge (No. 20180807.16)

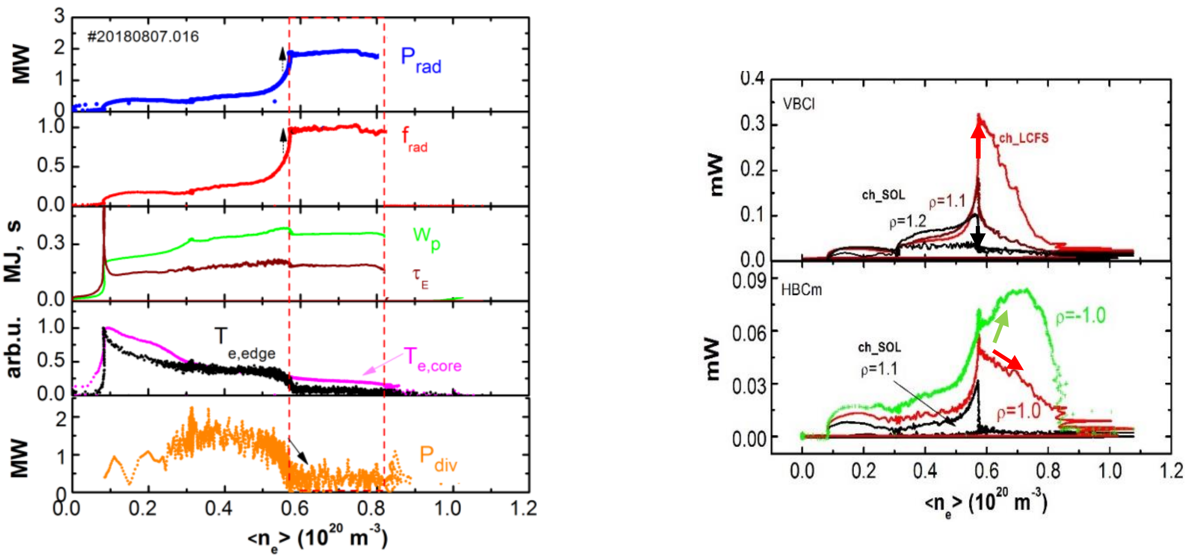

Fig. 1. (Left) Density dependence of parameters, such as P_{rad}, f_{rad}, W_p, τ_E, T_e, and P_{div} during density ramp-up for a 2 MW ECR-heated hydrogen plasma (No. 20180807.16). At a critical density of $<n_e> = 5.7\times10^{19} m^{-3}$, a transition to high radiation regime with f_{rad} ~1 (the detached plasma phase) occurs, shown by the dashed frame. (Right) At this critical density, signals of vertical bolometer channels (VBCl) viewing SOL (ρ >1) drops sharply while those viewing the LCFS increase rapidly; poloidal asymmetry becomes prominent indicted by rising of horizontal bolometer (HBCm) signal viewing ρ = -1 and decreasing of that viewing ρ = 1 shortly after detachment transition.

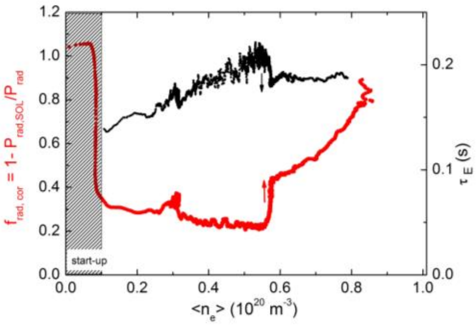

Fig. 2. The radiation power loss fraction inside the LCFS $f_{rad,core}$ (in red) and the energy confinement τ_E (in black) versus the plasma density for the discharge No. 20180807.16. Drop of τ_E occurs as $f_{rad,core}$ rapidly increases at a critical density of 5.7×10^{19} m^{-3}. The grey shaded area corresponds to the start-up phase of the plasma with total radiation from the region around the axis where ECRH power deposits.

in density ramp-up experiments. The density dependences of the parameters, such as the total radiated power loss P_{rad}, the radiation loss fraction, $f_{rad} = P_{rad}/P_{ECRH}$, the plasma stored energy W_p, the confinement time τ_E, calculated using $\tau_E = W_p/(P_{ECRH}\text{-}dW_p/dt)$, the (normalized) core and edge-temperatures T_e (measured by ECE diagnostic) and the total divertor heat load P_{div} are depicted in Fig. 1 (Left). As $\langle n_e\rangle$ increases to 5.7×10^{19}m^{-3}, a transition to high radiation regime with rapid increment of f_{rad} to ~1 occurs and P_{div} drops to ~0.2 MW (close to diagnostic resolution), simultaneously, indicating plasma detachment. Signals of bolometer channels viewing the SOL (ρ >1) drop sharply (see Fig. 1 (right)) while those viewing both the upper- and the lower side of the LCFS increase rapidly at first but then develop differently. Prominent poloidal asymmetry arises since the radiation from the lower part of LCFS (ρ = -1) increases further while that from the upper part (ρ = 1) declined. Further analysis shows that 1) at low-density, low-radiation regime, the radiation zone is predominantly located in the SOL, designated by a low value of $f_{rad,core}$ (~20%) for $\langle n_e\rangle < 5.7\times10^{19}$m^{-3}; 2) with increasing density, chord-brightness of SOL-channels weakens resulting in a reduction of radiation from SOL although the overall radiation level enhances. This implies an inward radial shift of the radiation zone; 3) for high-radiation regimes, the entire zone broadens in the radial direction and penetrates into the confined plasma with an enhanced level of $f_{rad,core}$. The variation of $f_{rad,core}$ with density is displayed in Fig. 2 (in red). It has been observed that τ_E drops as $f_{rad,core}$ increases rapidly from 20% to >40% during the detachment transition. This drop (even though not large) presents a degradation of the plasma performance (see Fig. 2 in black).

3.2 An exception: observation of co-enhancement of $f_{rad,core}$ and plasma performance

In a 4 MW ECR-heated hydrogen discharge with (overdosed) Fe-injections by TESPEL [10] for impurity transport study, we have, however, observed that the plasma energy W_p as well as the confinement time τ_E increase even though the radiation level $f_{rad,core}$ increases. Fig. 3 (Left) shows the time traces of the plasma parameters before, during and after the Fe-injections at t = 5 s. Both P_{rad} and $f_{rad,core}$ increases after Fe-injections due to line emissions from Fe-ions with high ionization stages (e.g. Fe^{23+} measured by spectrometers, not shown here). The SXR-bolometer has measured accordingly enhanced signals. The effective ion charge Z_{eff} increases from 1.5 to 2.0 estimated using the bremsstrahlung measurement. Divertor heat load P_{div} is reduced by a factor of 3. After Fe-injections, electron temperature $T_{e,0}$ (measured by the Thomson-scattering system) decreases; in contrast to this the ion temperature T_i measured by the XICS diagnostic [11-12] increases. The fluctuating density spectrum based on a Phase Contrast Imaging (PCI) technique [13] (see Fig.3 (right)) shows clear reduction of density fluctuation after Fe-injections at t ~ 5.1 s, indicating turbulent transport reduction. This phenomenon is similar to pellet enhanced confinement [14-15].

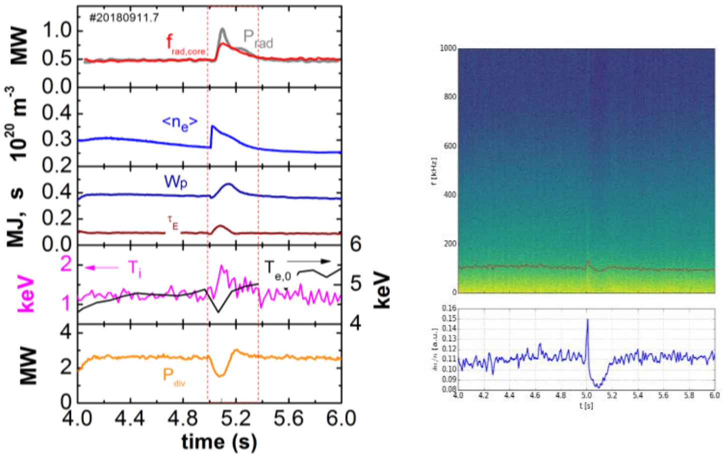

Fig. 3. (Left) Time traces of the plasma parameters before, during and after Fe-injections by TESPEL. (Right) The fluctuation density spectrum based on a Phase Contrast Imaging technique shows density fluctuation reduction after Fe- injections (at t ~5.1 s).

4. Summary and remarks

High-density, high-radiation regimes with plasma detachment have been observed at W7-X for both pre- and post-boronisation experiments. Examination of the plasma performance at detachment transition has been carried out. Correlation of $f_{rad,core}$ with degradation of both W_p and τ_E has been identified under the studied plasma conditions. However, co-enhancement of $f_{rad,core}$ with W_p and τ_E has been observed after Fe-injections. Systematic investigations concerning these topics are ongoing. Study of the underlying physics and exploration of the optimum operation windows of W7-X are addressed.

Acknowledgment

This work has been carried out within the framework of the EUROfusion Consortium and has received funding from the Euratom research and training programme under grant agreement No 633053. The views and opinions expressed herein do not necessarily reflect those of the European Commission.

References

[1] O. Grulke et al this conference
[2] D. Zhang et al. Rev. Sci. Instrum. **81,** 10E134 (2010).
[3]M. Krychowiak et al., Rev: Sci. Instrum. **87**,11D304 (2016).
[4] K. Rahbarnia, H. Thomsen, U. Neuner et al., Nuclear Fusion 58,096010 (2018)
[5]M. Jakubowski et al. Rev: Sci. Instrum. **89, 10E116**
[6]M. Hirsh et al. EPJ Web of Conferences 203, 03007 (2019)
[7]B. Buttenschön et al this conference
[8] D. Zhang et al Phys. Rev. Lett. (2019)
[9] O. Schmitz et al this conference
[10] N. Tamura et al this conference
[11]A. Langenberg et al. Review of Scientific Instruments, 89, 10G101 (2018)
[12] N.A. Pablant,et al. Physics Of Plasmas, 25, 022508 (2018)
[13] E.M. Edlund et al Rev. Sci. Instrum. 89, 10E105 (2018);
[14] J. Baldzuhn et al. to be published in Plasma Physics and Controlled Fusion, 2019
[15] S. Bozhenkov et al. this conference